

Parameters for Analysis on Distributed Circuit Properties of Etched Aluminum Oxide Film

Tatsuma YAMAMOTO*, Yoshitake YAMAMOTO*,
Hideki NISHIDA**, and Kiyotaka YASUHARA*

(Received November 1, 1977)

Synopsis

The distributed circuit properties based on pores in the etched aluminum oxide film of the electrolytic capacitor have been analysed by the mathematical equation. This paper proposes the selection and the determining method of the parameters appearing in the analysis.

1. Introduction

The etched aluminum oxide film or the sintered material, used in electrolytic capacitors, has countless microscopic pores. The circuit properties due to pores have been analysed by the transmission line model and its mathematical equation¹⁾²⁾. However, the problems to be studied on the selection and determination of the parameters appearing in analysis are yet left unsolved. The parameters, which cannot be determined experimentally, should be excepted from the analysis. This paper proposes on the selection and determination of the parameters, which can be simply obtained from the experimental data.

2. Results and Discussions

The simplified equivalent circuit of the electrolytic capacitor is generally given in Fig.1. L is a series inductance which is negligible

* Department of Electrical Engineering.

** Faculty of Education, Tottori University.

over the frequency range employed.

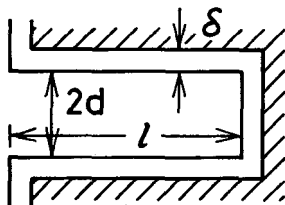
Z_{sol} is an impedance due to the electrolyte-separator combination.

Z_{sol} becomes the pure resistance R_0 when the separator paper is not used or the frequency is low. R' and C' are the interface impedance due to an aluminum cathode. Since an anode is not the metal, its interface impedance is small enough to neglect.

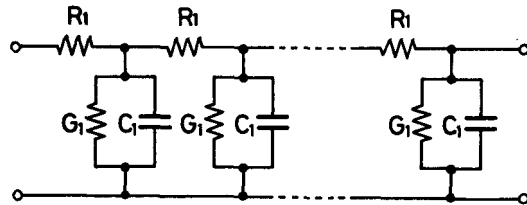
The test capacitors are made by pair of oxide films to make the nonpolar type. Accordingly, in the present study the interface impedance can be neglect. C_g is a capacitance formed with two foils, in which the electrolyte-separator combination is inserted as a dielectric, and C_g is small enough to neglect in comparison with C_s . R_s and C_s are an impedance based on the etched aluminum oxide film, and are determined by both dielectric properties of the film and distributed circuit properties due to a great many pores on the film.

Fig.2 shows the size of a pore and the transmission line model of circuit properties due to a pore. The diameter and length of a pore are $2d$ and l , respectively. The thickness of the film is δ . These geometric variables adopt the average values. $2d$, l and δ may be different according as an individual pore. However, the average values are usually applied in the analysis¹⁾²⁾. The series impedance $Z = R_s - j(1/\omega C_s)$ is expressed by Eq.(1), where the number of pores is N per pair of electrodes.

$$R_s = \frac{R_1 l/N}{\sqrt{2k}} f_R, \quad \frac{1}{\omega C_s} = \frac{R_1 l/N}{\sqrt{2k}} f_C \quad (1)$$



(a)



(b)

Fig.2 Configuration and circuit model of pore

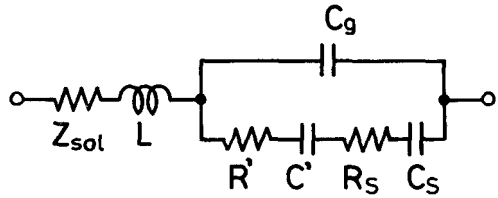


Fig.1 Equivalent circuit

where

$$f_R = \frac{\cos \frac{\phi}{2} \sinh 2A - \sin \frac{\phi}{2} \sin 2B}{\cosh 2A - \cos 2B}$$

$$f_C = \frac{\sin \frac{\phi}{2} \sinh 2A + \cos \frac{\phi}{2} \sin 2B}{\sinh 2A - \cos 2B} ,$$

$$A = \sqrt{2} k \cos \phi/2 , \quad B = \sqrt{2} k \sin \phi/2 ,$$

$$2k = [(R_1 \ell/N) |Y_\alpha|]^{1/2} , \quad |Y_\alpha| = [(G_2 \ell N)^2 + (\omega C_1 \ell N)^2]^{1/2} ,$$

$$\cot \phi = G_2 \ell N / \omega C_1 \ell N = \epsilon_2 / \epsilon_1 , \quad R_1 = \rho_1 / \pi d^2 ,$$

$$C_1 = 2\pi \epsilon_1 d / \delta , \quad G_2 = \omega \epsilon_2 2\pi d / \delta .$$

ρ_1 is the resistivity of the electrolyte and $\epsilon^* = \epsilon_1 - j\epsilon_2$ is the complex dielectric constant of the film. $|Y_\alpha|$ is a pseudo-admittance which is the quantity relating to a permeability of the film. Since the impedance is fortunately the function of only the parameters $R_1 \ell/N$, $G_2 \ell N$ and $C_1 \ell N$ at a given frequency, these parameters are called the fundamental parameters in this paper. The fundamental parameters are contained as a lump in Eq.(1), and are not separated; for example, as R_1 and ℓ/N , etc. and then the fundamental parameters are the macroscopic quantities defined for pair of electrodes. Next, the ratio of C_s at some standard low frequency f_0 Hz to that at the other arbitrary frequency f_n Hz is given as

$$C_{sr} = \frac{(C_s)_{f=f_n}}{(C_s)_{f=f_0}} = \frac{(f_c)_{f=f_0}}{\alpha_n (f_c)_{f=f_n}} , \quad (2)$$

where $\alpha_n = (f_n/f_0)^{1/2}$.

2.1 Films not having the dielectric loss

At first, we presume that the inherent dissipation factor

($\cot \phi = \epsilon_2/\epsilon_1$) of the film is zero. ϵ_1 becomes a constant value in this case. We can reduce Eq.(2) to the simple form:

$$C_{sr} = \frac{f_c(2b_0)}{\alpha_n f_c(2b_0 \alpha_n)}, \quad (3)$$

where $f_c(2b_0) = \lim_{G_2 \rightarrow 0} (f_c)_{f=f_0}$, $f_c(2b_0 \alpha_n) = \lim_{G_2 \rightarrow 0} (f_c)_{f=f_n}$,

$$2b = \lim_{G_2 \rightarrow 0} 2k = \sqrt{6\omega C_{s0} R_{s0}}$$

$$= \sqrt{4\omega(\ell^2/d)C\rho_1}, \quad 2b_0 = (2b)_{f=f_0},$$

$$C = \epsilon/\delta, \quad R_{s0} = R_1 \ell/3N, \quad C_{s0} = C_1 \ell N.$$

Since $\lim_{\substack{\omega \rightarrow \infty \\ G_2 \rightarrow 0}} f_R = \lim_{\substack{\omega \rightarrow \infty \\ G_2 \rightarrow 0}} f_C = 1$ is obtained at high frequency, R_s and $1/\omega C_s$ are proportional to $\omega^{-1/2}$. Then, $\lim_{\substack{\omega \rightarrow 0 \\ G_2 \rightarrow 0}} R_s = R_{s0}$ and $\lim_{\substack{\omega \rightarrow 0 \\ G_2 \rightarrow 0}} C_s = C_{s0}$ are obtained at low frequency, where R_{s0} and C_{s0} are constant values. The analysis for the sintered material also is almost the same³⁾. In the analyses to date, the adequate considerations relating to the selection and determination of the parameters to describe Eq.(1) have hardly been given. In case of $G_2 = 0$, R_{s0} and C_{s0} ²⁾ or ρ_1 , C , and ℓ/\sqrt{d} ¹⁾ were selected by each author as parameters. Although R. H. Broadbent¹⁾ has determined as $\ell/\sqrt{d} = 0.16$, the determination of C was obscure. The experimental determination of the microscopic parameters (C and ℓ/\sqrt{d}) is not simple, and is hardly performed in practice. K. Nishitani²⁾ described the experimental determination of R_{s0} and C_{s0} . However, the experimental determination of R_{s0} is very difficult because of reasons as follows: (1) since the test sample is capacitive essentially, the resistive component R_{s0} at low frequency can hardly be measured, and (2) although R_s is obtained by subtracting the electrolytic resistance R_0 from the total series resistance, R_s is not simply determined because the main part of the total series resistance is almost R_0 .

To settle these problems, Eq.(3) can be used effectively. C_{sr} is a transcendental function of $2b_0$, so that $2b_0$ can not be expressed

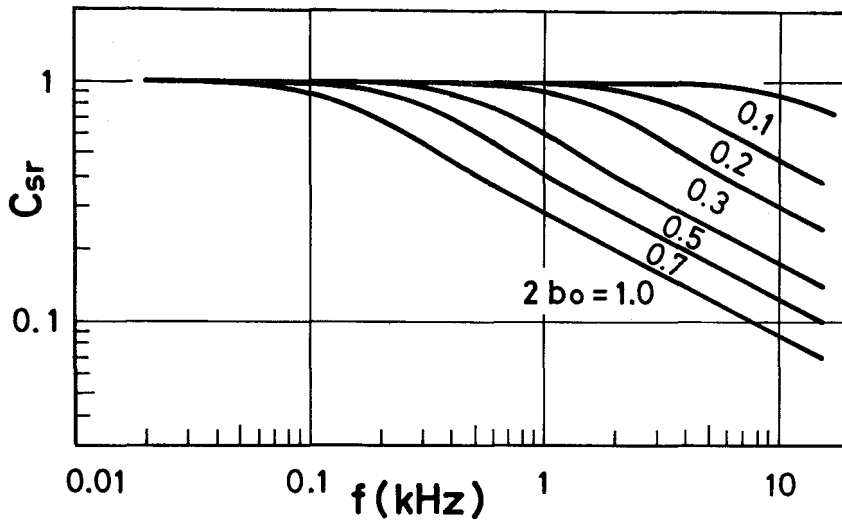
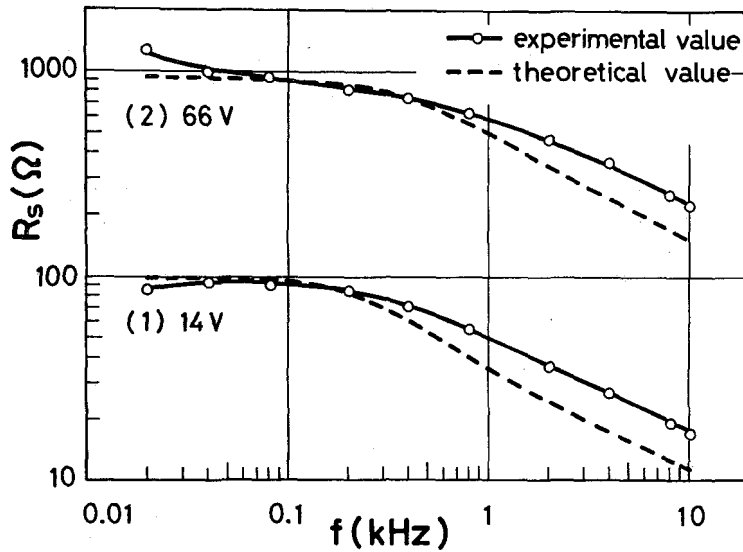
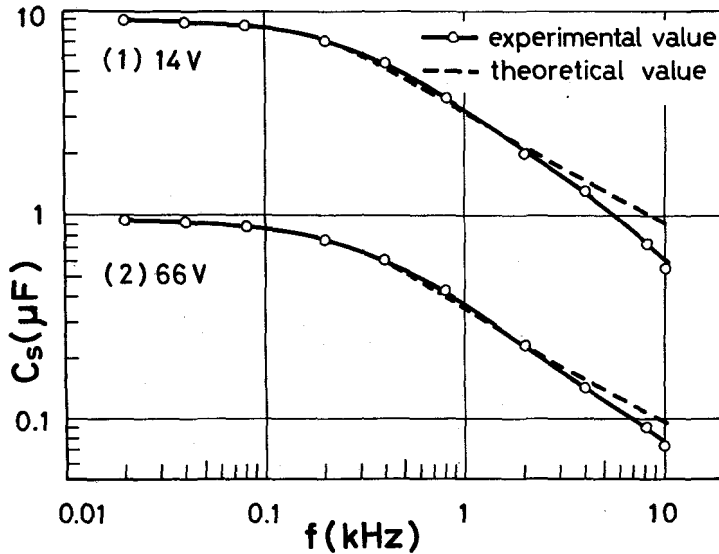


Fig.3 Theoretical curves of C_{sr} vs. frequency

analytically using the capacitances at two frequencies. Therefore, the determination of $2b_0$ is performed by means of a graphical solution as follows: Since C_{sr} is theoretically calculated as a function of $2b_0$ and various values of α_n ($n = 1, 2, \dots$), the graph as shown in Fig.3 can be beforehand described. On the other hand, C_{sr} also can be experimentally determined as the ratio between two capacitance values at f_0 and f_n Hz. Therefore, when an experimental curve agrees optimally with a theoretical curve in Fig.3, the unknown quantity $2b_0$ is determined as the value of $2b_0$ belonging to its theoretical curve. Next the constant value of C_s obtained at very low frequency gives the value of C_{s0} . Thus the new fundamental parameters ($R_1 \ell/N$ and $C_1 \ell/N$) are simply determined from $2b_0$ and C_{s0} , as $C_1 \ell/N = C_{s0}$ and $R_1 \ell/N = (2b_0)^2 / 4\pi f_0 C_{s0}$. It is a remarkable feature that these parameters are obtained from the frequency characteristic of the capacitance alone. The difficulty of the experimental determination of R_{s0} is illustrated by the following example. The break frequency, given as the frequency at the bend point of the curve of C_{sr} , decreases with the increase of $2b_0$ or ρ_1 as shown in Fig.3. Therefore, 4% boric acid solution ($H_3BO_3 = 4\%$, $H_2O = 96\%$, resistivity $277\Omega \cdot m$ at $17^\circ C$) having large value of ρ_1 was used, because the distributed properties appear even at lower frequency and hence observations are simply made. Films made at formative voltages 14V and 66V were used as test samples. To make the nonpolar sample, a capacitor was made by pair of films (effective area: $1cm^2$, distance between two films: 0.15mm). The solid lines in Fig.4



(a)



(b)

Fig.4 R_s and C_s vs. frequency

show experimental results on distributed properties, and the dotted lines are theoretical curves calculated from Eq.(1) ($G_2 = 0$ in this case), using $R_1 \ell/N$ (14V --- 291Ω , 66V --- 2720Ω) and $C_1 \ell/N$ (14V --- $8.77\mu\text{F}$, 66V --- $0.936\mu\text{F}$) determined by the above process. In low

frequency, although the adequate agreement in capacitance curves is read, the dotted lines of the resistance agree roughly with solid lines. Here 20Hz was used as f_0 . The phase angles $\tan^{-1}1/\omega C_S(R_0+R_S)$ show about 57° (14V) and 79° (66V) at 20Hz, so that the experimental determination of R_S is considerably difficult even in these special examples. Hence the experimental curves of R_S do not agree adequately with theoretical curves. Since the phase angle of the usual electrolytic capacitor becomes about 90° in low frequency, the experimental determination of R_{S0} is more difficult in comparison with the above examples.

2.2 Film having the dielectric loss

Next, we presume that the inherent dissipation factor of the film is not zero. In this case, the series capacitance C_S in low frequency is not constant, but a function of frequency, so that the existence of the dissipation can be simply verified, and then the large resistance due to the dissipation raises the accuracy of the measurement of resistance. In low frequency, since $|Y_d|$ is small, $R_1 \ell/N \ll 1/|Y_d|$, $2A \ll 1$, and $2B \ll 1$ are obtained and moreover we obtain $Z \doteq 1/Y_d$ from Eq.(1). Namely, the distributed properties due to pores hardly appear, and on the other hand the dielectric properties of the film become a dominating factor. The vector locus of G_p/ω and C_p obtained from the perfect admittance $Y = G_p + j\omega C_p = 1/Z$ is shown by the mark O in Fig.5, where G_p and C_p can be calculated using the well-known series-parallel

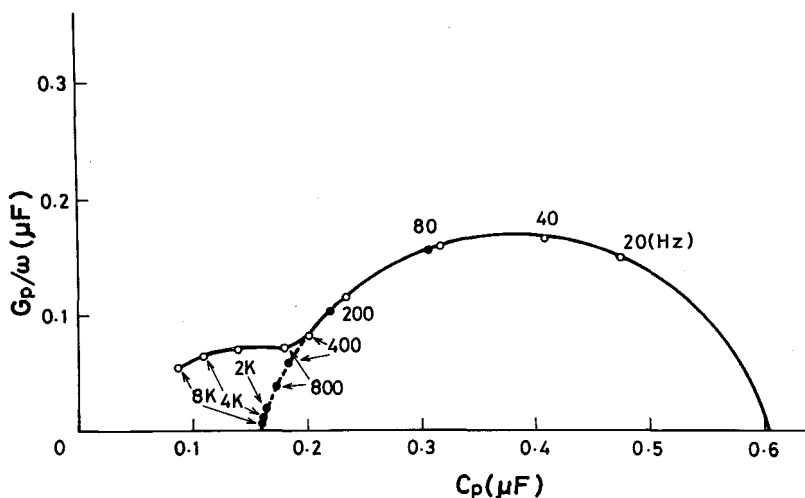


Fig.5 Vector locus of G_p/ω and C_p

transformation formula of the impedance. This locus is obtained on film of the test sample made at formative voltage 220V, and deviates from the circular arc in high frequency because of appearance of the distributed properties. In low frequency, since $Y = Y_d$ is obtained, G_p/ω and C_p are proportional to ϵ_2 and ϵ_1 , respectively. It can be read that this locus is satisfied with the Cole-Cole circular arc law. The fundamental parameters $G_2 \ell N \doteq G_p$ and $C_1 \ell N \doteq C_p$ at some low frequencies are determined from Fig.5. To obtain the parameters in high frequency, this locus, however, must be extrapolated, using the Cole-Cole circular arc law, as shown by the mark ● in Fig.5. Thus $G_2 \ell N = 0.0175, 0.131, 0.347, 0.303\text{mS}$, and $C_1 \ell N = 0.495, 0.22, 0.165, 0.161\mu\text{F}$ are obtained at 0.02, 0.2, 2, and 8kHz, respectively. Since the parameters $G_2 \ell N$ and $C_1 \ell N$ at f_0 and f_n Hz can be determined, the right term of Eq.(2) becomes a function of $R_1 \ell/N$ alone. Therefore, if the left term (i.e. experimental value) of Eq.(2) is given, $R_1 \ell/N$ can be calculated using a computer technique. The calculated mean value of $R_1 \ell/N$ on the sample of Fig.5 is 450Ω , as $f_0 = 20\text{Hz}$, and using this value, relative errors ($100 \times (\text{experimental value of } C_{sr} - \text{calculated value of } C_{sr}) / \text{calculated value of } C_{sr}$) are 13.9, 18.8, 9.8, 1.05, and -3.34% at $f_n = 400, 800, 2k, 4k, \text{ and } 8\text{kHz}$, respectively. The large errors in low frequency arise from the dominant dielectric properties, in comparison with the distributed properties, as mentioned above.

Since the macroscopic fundamental parameters $R_1 \ell/N$, $G_2 \ell N$, and $C_1 \ell N$, and their determination method are proposed, the distributed circuit properties due to pores on the film of the electrolytic capacitor will be more rationally analysed, or the obscurity appearing in the past analysis will disappear by the present study.

References

- 1) R. H. Broadbent: "Alternating-Current Properties of Aluminum Foil Electrolytic Capacitors", *Electrochemical Technology*, 6(1968), 5-6, 163-166
- 2) K. Nishitani: "The AC Properties of Electrolytic Capacitors Forming Distributed Networks", *J. of Electrical Engineering, Japan*, 89(1969), 970, 1333-1342
- 3) J. Vergnolle: "Distributed Network Analysis of Porous Electrode Capacitors", *J. of Electrochemical Society*, 111(1964), 7, 799-804